SIAM J. NUMER. ANAL.
Vol. 25, No. 2, April 1988

ON GODUNOV-TYPE METHODS FOR GAS DYNAMICS*

BERND EINFELDT†

Abstract. In this paper we describe a new approximate Riemann solver for compressible gas flow. In contrast to previous Riemann solvers, where a numerical approximation for the pressure and the velocity at the contact discontinuity is computed, we derive a numerical approximation for the largest and smallest signal velocity in the Riemann problem. Having obtained the numerical signal velocities, we use theoretical results by Harten, Lax and van Leer to obtain the full approximation.

A stability condition for the numerical signal velocities is derived. We also demonstrate a relation between the signal velocities and the dissipation contained in the corresponding Godunov-type method.

The computation of signal velocities for a general (convex) equation of state is discussed. Numerical results for the one- and two-dimensional compressible gas dynamics equations are also given.

Key words. Riemann solver, Godunov-type methods, hyperbolic conservation laws, gas dynamics, equation of state

AMS(MOS) subject classifications. 65M05, 65M10, 76M05

1. Introduction.

In the last several years Godunov-type methods have been applied successfully for the calculation of inviscid compressible flow. In practice, these methods are characterized by their robustness and their usefulness in computing flows with very complicated shock structures.

Godunov [7] used the nonlinear Riemann problem as a "building block" for his numerical method. This allows a self-operating treatment of weak and strong shock waves. The numerical solution represents shocks nearly optimally thin; a monotone profile over one to three computational cells without nonphysical oscillations is typical. From the theoretical point of view, Godunov's method is an extension of the classical Courant–Isaacson–Rees scheme [10]. The underlying physical picture of Godunov's method is useful for the interpretation of certain schemes and in construction of new ones.

The recent interest in Godunov-type methods was engendered by van Leer, who realized the importance of Godunov's method and invented a second-order extension. Further developments along this line were made by Colella and Woodward [1], Colella [2] and Woodward, Colella, Fryxell and Winkler [25]. A comparison of some of these Godunov-type methods with more classical methods can be found in [26].

The disadvantage of Godunov's method and its higher-order extension is the difficulty of solving the nonlinear Riemann problem exactly, especially for materials with complex equations of state. The exact solution of the Riemann problem requires an iterative procedure, which leads to relatively complex and time-consuming numerical codes. Since computational efficiency is a major requirement for applied numerical methods, this has restricted the extensive applications of Godunov-type methods.

To overcome this drawback, several approximations to the Riemann problem have been developed. For ideal (polytropic) equations of state there are, by now, particular approximate "Riemann solvers" available; among them are the methods developed by Osher and Solomon [15] and Roe [18] and Pandolfi [17]. These linear approximations are also of interest in the field of aerodynamics where they provide a foundation

* Received by the editors January 5, 1987; accepted for publication April 14, 1987. This research is part of a joint task conducted by the Sonderforschungsbereich 27 "Wellen fokussierung" supported by the Deutsche Forschungsgemeinschaft.

† Institut für Geometrie und Praktische Mathematik der RWTH Aachen, Templegraben 55, 5100 Aachen, West Germany.

for the construction of more elaborate schemes [19], [20]. More analytical effort is required if a general equation of state is considered. So far, only two Riemann solvers have been developed in this case. One iterative method is by Colella and Glaz [3] and a second explicit method is by Dukowicz [5]. It is interesting to note that Dukowicz derived his Riemann solver by establishing a relationship to the artificial shock viscosity methods.

In this paper we describe a new approximate Riemann solver for compressible gas flow. In contrast to previous Riemann solvers, where a numerical approximation for pressure and velocity at the contact discontinuity is computed, we derive a numerical approximation for the largest and smallest signal velocity in the Riemann problem. Having obtained the numerical signal velocities we use theoretical results by Harten, Lax and van Leer [10] to obtain the full approximation. This new Riemann solver keeps the computing time extremely low, while retaining the essential properties of Godunov's method and provides, therefore, an attractive alternative on which to construct higher-order extensions.

The organization of this paper is as follows: In §§ 2 and 3 we describe the theoretical foundations of the Riemann solver. The stability and dissipation of the corresponding Godunov-type method are discussed in § 4. In § 5 we show how to obtain simple numerical approximations for the signal velocities. Numerical results for the one- and two-dimensional compressible gas dynamics equations are given in § 6. Section 7 contains our conclusion.

A comparison with Godunov's method [7] and Roe's scheme [18] is also contained in §§ 4 and 6. This makes this article, to a certain extent, a review paper.

2. Preliminaries.

A. Conservation equation. We consider the (Euler) equations for an inviscid compressible flow. The conservation form of these equations in one Cartesian space variable is

$$\frac{\partial v}{\partial t}+\frac{\partial f(v)}{\partial x}=0, \tag{2.1}$$

where the conserved quantities v and fluxes f are:

$$v=\begin{pmatrix}\rho\\ m\\ e\end{pmatrix}, \qquad f(v)=\begin{pmatrix}m\\ m^2/\rho+p\\ m/\rho(e+p)\end{pmatrix}. \tag{2.2}$$

Here, ρ is the density, $m=\rho u$ is the momentum per unit length and $e=\rho\varepsilon+\frac{1}{2}\rho u^2$ is the total energy per unit length. The physical variables u and ε are the velocity and the internal energy per unit mass. The pressure p is related to the conserved quantities through the equation of state

$$p=p(\tau, \varepsilon), \tag{2.3}$$

where $\tau=1/\rho$ is the specific volume. In the case of an ideal equation of state we have

$$p=(\gamma-1)\frac{\varepsilon}{\tau}. \tag{2.4}$$

In this paper we concentrate on an ideal equation of state and indicate a possible extension to general equations of state. General convex equations of state will be considered in a future paper.

B. The Riemann problem. The Riemann problem is an initial value problem for (2.1) with the initial data

$$v(x, 0) = \begin{cases} v_l & \text{for } x < 0, \\ v_r & \text{for } x > 0. \end{cases}$$

A detailed discussion of the Riemann problem is given by Courant and Friedrichs [4] and in [22], [6] for an ideal equation of state.

The solution to the Riemann problem consists of four constant states separated by three elementary waves. The backward and forward facing wave is either a rarefaction or shock wave. The center wave is always a contact discontinuity (Fig. 1). The exact solution is obtained by an iterative method described in [3]. The solution to the Riemann problem incorporates a large amount of information about the physical system that is modeled by (2.1). It includes, for example, the directions and strength of the disturbances that emerge from the nonlinear interaction of two constant states. For that reason, the solution of the Riemann problem is a natural "building block" for the construction of upstream differencing schemes.

C. Godunov's method. We divide the time into intervals of length τ and let Δ be the spatial increment. The solution is to be evaluated at time $t^n = n\tau$, where n is a nonnegative integer at the spatial increments $x_i = i\Delta$, $i = 0, \pm 1, \pm 2, \cdots$. Let v_i^n approximate the cell average

$$\frac{1}{\Delta} \int_{x_{i-1/2}}^{x_{i+1/2}} v(x, t^n)\, dx$$

where $x_{i+1/2} = (i+1/2)\Delta$.

In Godunov's upstream differencing scheme [7], the fluid is described as a sequence of cell-averaged conserved quantities ρ_i^n, m_i^n, e_i^n. The cell averages are advanced in time by first solving a Riemann problem at each cell interface. The averages $v_i^{n+1} = (\rho_i^{n+1}, m_i^{n+1}, e_i^{n+1})$ at the next time level $t^{n+1} = t^n + \tau$ are obtained by averaging over a cell $((i-1/2)\Delta, (i+1/2)\Delta)$; i.e.,

$$v_i^{n+1} = \frac{1}{\Delta} \int_0^{\Delta/2} \omega_{i-1/2}^n(x/\tau)\, dx + \frac{1}{\Delta} \int_{-\Delta/2}^0 \omega_{i+1/2}^n(x/\tau)\, dx \tag{2.5}$$

where $\omega_{i+1/2}^n(x - x_{i+1/2}/(t - t^n))$ is the solution to the Riemann problem at the cell interface $x_{i+1/2} = (i+1/2)\Delta$ at time t^n (Fig. 2). Equation (2.5) can be rewritten as

$$v_i^{n+1} = v_i^n - \frac{\tau}{\Delta}(g_{i+1/2}^n - g_{i-1/2}^n), \tag{2.6}$$

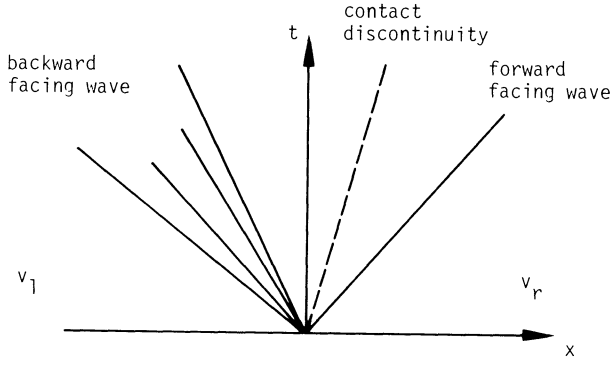

FIG. 1. *The solution of the Riemann problem in physical space.*

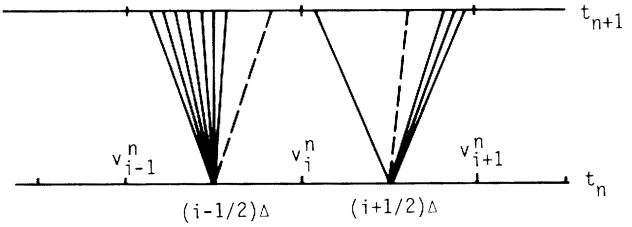

FIG. 2. *Godunov's method in physical space.*

where the numerical flux $g^n_{i+1/2}$ is given by

$$g^n_{i+1/2} = g(v^n_i, v^n_{i+1}) = f(\omega^n_{i+1/2}(0)). \tag{2.7}$$

More details can be found in the paper by Harten, Lax and van Leer [10].

3. The Riemann solver. The solution $\omega_{i+1/2}((x - x_{i+1/2})/(t - t^n))$ of the Riemann problem

$$\begin{aligned} &v_t + f(v)_x = 0, \\ &v(x, 0) = \begin{cases} v_i & \text{for } x < x_{i+1/2}, \\ v_{i+1} & \text{for } x > x_{i+1/2} \end{cases} \end{aligned} \tag{3.1}$$

at the cell interface $x_{i+1/2}$, depends only on the state v_i, v_{i+1} and the ratio $(x - x_{i+1/2})/t$. For convenience, we assume that $t^n = 0$ and omit the subscript n. Furthermore,

$$\omega_{i+1/2}\left(\frac{x'}{t}\right) = \begin{cases} v_i & \text{for } x' < a^l_{i+1/2} t, \\ v_{i+1} & \text{for } x' > a^r_{i+1/2} t \end{cases} \tag{3.2}$$

where $x' = x - x_{i+1/2}$ and $a^l_{i+1/2}$, $a^r_{i+1/2}$ are the smallest and largest physical signal velocity, respectively. The HLL-Riemann solver, theoretically discussed by Harten, Lax and van Leer [10], extracts the information about the signal velocities from the full Riemann problem. It consists of three constant states, i.e.,

$$\omega_{i+1/2}(x'/t) = \begin{cases} v_i & \text{for } x' < b^l_{i+1/2} t, \\ v_{i+1/2} & \text{for } b^l_{i+1/2} t < x' < b^r_{i+1/2} t, \\ v_{i+1} & \text{for } b^r_{i+1/2} t < x'. \end{cases} \tag{3.3}$$

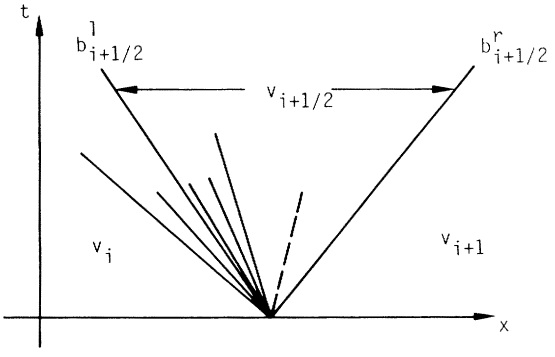

FIG. 3. *The approximate solution* (3.3) *of the Riemann problem.*

Here, $b^l_{i+1/2}$ and $b^r_{i+1/2}$ are Lipschitz-continuous approximations to the smallest and largest physical signal velocities (Fig. 3). The average state $v_{i+1/2}$ is defined such that the Riemann solver is consistent with the integral form of the conservation law, i.e.,

$$\int_{-\Delta/2}^{+\Delta/2} \omega_{i+1/2}(x'/t)\, dx' = \Delta/2(v_i + v_{i+1}) - \tau f(v_{i+1}) + \tau f(v_i), \tag{3.4}$$

for $\Delta/2 > \tau \max\{|b^l_{i+1/2}|, |b^r_{i+1/2}|\}$. Having computed the approximate Riemann solver at the cell interfaces, we obtain the cell averages at the next time level similar to (2.5):

$$v^1_i = 1/\Delta \int_0^{\Delta/2} \omega^0_{i-1/2}(x'/\tau)\, dx' + 1/\Delta \int_{-\Delta/2}^{0} \omega^0_{i+1/2}(x'/\tau)\, dx'. \tag{3.5}$$

This again can be rewritten in the conservation form

$$v^1 = v^0_i - \lambda(g^0_{i+1/2} - g^0_{i-1/2}), \tag{3.6}$$

with the numerical flux function

$$\begin{aligned} g_{i+1/2}(v_i, v_{i+1}) &= f(v_i) \quad \text{for } 0 < b^l_{i+1/2} \\ &= \frac{b^r_{i+1/2} f(v_i) - b^l_{i+1/2} f(v_{i+1})}{b^r_{i+1/2} - b^l_{i+1/2}} + \frac{b^l_{i+1/2} b^r_{i+1/1}}{b^r_{i+1/2} - b^l_{i+1/2}}(v_{i+1} - v_i) \\ &\qquad \text{for } b^l_{i+1/2} < 0 < b^r_{i+1/2} \\ &= f(v_{i+1}) \quad \text{for } b^r_{i+1/2} < 0. \end{aligned} \tag{3.7}$$

This again can be combined into a single formula:

$$g_{i+1/2} = \frac{b^+_{i+1/2} f(v_i) - b^-_{i+1/2} f(v_{i+1})}{b^+_{i+1/2} - b^-_{i+1/2}} + \frac{b^+_{i+1/2} b^-_{i+1/2}}{b^+_{i+1/2} - b^-_{i+1/2}}(v_{i+1} - v_i), \tag{3.7'}$$

where $b^+_{i+1/2} = \max(0, b^r_{i+1/2})$ and $b^-_{i+1/2} = \min(0, b^l_{i+1/2})$. The definition (3.3) of the Riemann solver differs from the one given in [10]. In contrast to the original version, we do not assume that the numerical signal velocities $b^l_{i+1/2}$, $b^r_{i+1/2}$ are lower and upper bounds for the physical signal velocities $a^l_{i+1/2}$, $a^r_{i+1/2}$. Stability bounds for the numerical signal velocities will be derived in the next section.

Suppose that the solution of the Riemann problem consists of a single shock. In this case the exact solution is

$$u(x, t) = \begin{cases} v_i & \text{for } x' < st, \\ v_{i+1} & \text{for } st < x', \end{cases} \tag{3.8}$$

where s is the speed of the propagation of the shock. Suppose further that the algorithm for calculating the numerical signal velocities is such that it furnishes

$$b^l_{i+1/2} = s \quad \text{for a backward facing shock,} \tag{3.9a}$$

$$b^r_{i+1/2} = s \quad \text{for a forward facing shock.} \tag{3.9b}$$

It then follows from the equality of $v_{i+1/2}$, with the mean value of the exact solution, that (3.3) is the exact solution (3.8).

Let v_i and v_{i+1} be connected by a single contact discontinuity. The exact solution is again (3.8) with the shock speed replaced by the characteristic velocity $u_i = u_{i+1} = u$. In general,

$$b^l_{i+1/2} < u < b^r_{i+1/2}. \tag{3.10}$$

Thus, the Riemann solver (3.3) spreads the contact discontinuity and is a rather rough approximation to the exact solution.

Next we show how to modify the Riemann solver (3.3) to obtain a more accurate approximation of a contact discontinuity.

The information of the contact discontinuity is buried in the average state $v_{i+1/2}$. A contact wave is a weak solution of (2.1) of the form

$$v(x, t) = \omega(x, t)(1, u, \tfrac{1}{2}u^2)^T, \tag{3.11}$$

where u is the constant velocity of propagation of the wave. We therefore recover the information about the contact discontinuity, by modifying the average state $v_{i+1/2}$ in (3.3) by

$$\omega_{i+1/2} = \begin{cases} v_i & \text{for } x'/t < b^l_{i+1/2}, \\ v_{i+1/2} + \delta_{i+1/2}(x - \bar{u}_{i+1/2}t)\eta^2_{i+1/2}R^2_{i+1/2} & \text{for } b^l_{i+1/2} < x'/t < b^r_{i+1/2}, \\ v_{i+1} & \text{for } b^r_{i+1/2} < x'/t. \end{cases} \tag{3.12}$$

Here

$$R^2_{i+1/2} = (1, \bar{u}_{i+1/2}, \tfrac{1}{2}\bar{u}^2_{i+1/2})^T, \tag{3.13a}$$

and

$$\eta^2_{i+1/2} = l^2_{i+1/2}(v_{i+1} - v_i) \tag{3.13b}$$

with

$$l^2_{i+1/2} = \left(1 - \frac{\gamma - 1}{2}\frac{\bar{u}^2_{i+1/2}}{\bar{c}^2_{i+1/2}}, (\gamma - 1)\frac{\bar{u}_{i+1/2}}{\bar{c}^2_{i+1/2}}, \frac{(1-\gamma)}{\bar{c}^2_{i+1/2}}\right). \tag{3.13c}$$

$\delta_{i+1/2}$ is a parameter which will be specified in the next section. Observe that $R^2_{i+1/2}$ is the second eigenvector of the Jacobian matrix df and that $\eta^2_{i+1/2}$ is an approximate value for the projection from $v_{i+1} - v_i$ onto this eigenvector. $\bar{u}_{i+1/2}$ and $\bar{c}_{i+1/2}$ are numerical approximations of the velocity and the sound speed at the contact discontinuity. We define

$$\bar{u}_{i+1/2} = \frac{b^r_{i+1/2} + b^l_{i+1/2}}{2}, \tag{3.14a}$$

$$\bar{c}_{i+1/2} = \frac{b^r_{i+1/2} - b^l_{i+1/2}}{2}. \tag{3.14b}$$

The approximate solution (3.12) is thus completely defined by the numerical signal velocities. The modification of the average state $v_{i+1/2}$ does not change the integral (3.4). Therefore the Riemann solver (3.12) remains in conservation form. The numerical flux of the corresponding Gundov-type method is defined by

$$\begin{aligned} h_{i+1/2} &= f(v_i) - \frac{1}{\tau}\int_{-\Delta/2}^{0} \omega_{i+1/2}(x'/\tau)\, dx' + \frac{\Delta}{2}v_i \\ &= g_{i+1/2} - b^+_{i+1/2}b^-_{i+1/2}\frac{\tau}{2}\delta_{i+1/2}\eta^2_{i+1/2}R^2_{i+1/2}, \end{aligned} \tag{3.15}$$

where $g_{i+1/2}$ is the numerical flux (3.7).

4. Dissipation and stability. The resolution of a shock wave or contact discontinuity is largely determined by the numerical dissipation of the difference scheme. In this section we will study the dissipation for the Godunov-type methods described here.

The numerical flux function (3.7) may also be written in the form

$$g_{i+1/2} = \tfrac{1}{2}[f(v_i) + f(v_{i+1}) - Q_{i+1/2}(v_{i+1} - v_i)], \tag{4.1}$$

where the numerical viscosity-matrix $Q_{i+1/2}$ is defined by

$$Q_{i+1/2}=\frac{b^r_{i+1/2}+b^l_{i+1/2}}{b^r_{i+1/2}-b^l_{i+1/2}}A_{i+1/2}-2\frac{b^r_{i+1/2}b^l_{i+1/2}}{b^r_{i+1/2}-b^l_{i+1/2}}I. \tag{4.2}$$

Here the matrix $A_{i+1/2}$ is a Roe-type linearization which has real eigenvalues $\alpha^k_{i+1/2}$, a complete set of eigenvectors and satisfies

$$f(v_{i+1})-f(v_i)=A_{i+1/2}(v_{i+1}-v_i). \tag{4.3}$$

The existence of a Roe-type linearization follows from the existence of an entropy function for (2.1) (see [10]).

A necessary condition for stability is that the viscosity matrix $Q_{i+1/2}$ has nonnegative eigenvalues. The eigenvalues of $Q_{i+1/2}$ are

$$\sigma^k_{i+1/2}=\frac{b^+_{i+1/2}(\alpha^k_{i+1/2}-b^-_{i+1/2})-b^-_{i+1/2}(b^+_{i+1/2}-\alpha^k_{i+1/2})}{b^+_{i+1/2}-b^-_{i+1/2}} \tag{4.4}$$

$$(k=1,\cdots,3)$$

where $\alpha^k_{i+1/2}$ denotes the eigenvalue of $A_{i+1/2}$. Thus, we obtain a necessary stability condition for the signal velocities

$$\sigma^k_{i+1/2}\geqq 0, \tag{4.5}$$

which is satisfied if

$$b^-_{i+1/2}\leqq\alpha^k_{i+1/2}\leqq b^+_{i+1/2}\quad\text{for } k=1,\cdots,3. \tag{4.6}$$

If the strong inequality holds in (4.6), then the scheme (3.6) is dissipative of order two. Since $g_{i+1/2}(v,v)=f(v)$, the scheme is accurate of order one and for a linear flux function f, L_2-stability follows from the Kreiss theorem [23, Thm. 3.3].

A stronger TVD-type condition for the viscosity matrix $Q_{i+1/2}$ is

$$\sigma^k_{i+1/2}\geqq|\alpha^k_{i+1/2}|\qquad(k=1,\cdots,3). \tag{4.7}$$

For linear f or scalar nonlinear f this requirement implies that a scheme (3.6) in conservation form is total variation diminishing (TVD), under the CFL restriction

$$\lambda\sigma_{i+1/2}\leqq 1 \tag{4.8}$$

(see Harten [8]). TVD difference schemes are monotonicity preserving, which guarantees that the scheme does not generate spurious oscillations. A short calculation shows that the stronger condition (4.7) holds if and only if the signal velocities satisfy the inequalities (4.6).

Suppose that the solution of the Riemann problem consists of a single shock. In this case the exact solution is (3.8), where the shock speed satisfies the Rankine-Hugoniot condition

$$f(v_i)-f(v_{i+1})=s(v_i-v_{i+1}). \tag{4.9}$$

From (4.3) and (4.9) it follows that the shock speed s is an eigenvalue $\alpha^k_{i+1/2}$ ($k=1$ or 3) of the Roe linearization $A_{i+1/2}$. Therefore, for a backward facing shock the only dissipation is introduced through the first eigenvalue $\sigma^1_{i+1/2}$ of the viscosity matrix $Q_{i+1/2}$. We have

$$\sigma^1_{i+1/2}\geqq|s|, \tag{4.10}$$

where the equality sign holds for $b^l_{i+1/2} = s$. This shows that the least amount of numerical dissipation is introduced in the method (3.6), (3.7) if

$$b^l_{i+1/2} = s = \alpha^1_{i+1/2}.$$

A similar statement holds for a forward facing shock.

In the case of a stationary shock, we may have that $\sigma^k_{i+1/2} = |s| = 0$ for $k = 1$ or 3 and the numerical viscosity term in (4.1) vanishes. The lack of numerical dissipation allows the perfect resolution of stationary shocks, i.e., (3.8) with $s = 0$ is a steady solution of the numerical scheme. On the other hand, the scheme may admit a stationary nonphysical discontinuity. To avoid this we may modify the numerical signal speeds by

$$\hat{b}^l_{i+1/2} = \min\,(b^l_{i+1/2}, \lambda_1), \tag{4.11a}$$

$$\hat{b}^r_{i+1/2} = \max\,(b^r_{i+1/2}, \lambda_3), \tag{4.11b}$$

where $\lambda_1 = \mu_i - c_i$ and $\lambda_3 = u_{i+1} + c_{i+1}$ are the first and third eigenvalues of the Jacobian $df(v_i)$, $df(v_{i+1})$, respectively. Since the entropy inequality

$$\lambda_k(u_r) < s < \lambda_k(u_l) \qquad (k = 1, 3) \tag{4.12}$$

holds [22], we observe that the modification (4.11) does not effect the resolution of a shock wave. For a nonphysical discontinuity the inequality in (4.12) is reversed. In this case the signal velocities (4.11) introduce enough numerical dissipation to avoid the occurrence of a nonadmissible discontinuity.

Now suppose that v_i and v_{i+1} are connected by a contact discontinuity. The exact solution is again (3.8), with the shock speed s replaced by the characteristic speed $u = u_l = u_r$. From (4.3) and (4.9) it follows that u is equal to the second eigenvalue $\alpha^2_{i+1/2}$ of $A_{i+1/2}$. The only dissipation is introduced through the second eigenvalue of the viscosity matrix $Q_{i+1/2}$. Since

$$b^l_{i+1/2} \leqq \alpha^1_{i+1/2} < \alpha^2_{i+1/2}, \tag{4.13a}$$

$$\alpha^2_{i+1/2} < \alpha^3_{i+1/2} \leqq b^r_{i+1/2} \tag{4.13b}$$

we have

$$\begin{aligned} &\sigma^2_{i+1/2} = |\alpha^2_{i+1/2}| = |u| \quad \text{for } b^+_{i+1/2} b^-_{i+1/2} = 0, \\ &\sigma^2_{i+1/2} > |\alpha^2_{i+1/2}| = |u| \quad \text{otherwise.} \end{aligned} \tag{4.14}$$

Therefore, the numerical dissipation for a nearly stationary contact discontinuity is larger than it is for Godunov's method.

Now consider the modified numerical flux function (3.15). If we assume that

$$\bar{u}_{i+1/2} = \frac{b^l_{i+1/2} + b^r_{i+1/2}}{2} = \alpha^2_{i+1/2} \tag{4.15}$$

and represent $v_{i+1} - v_i$ in terms of the right eigenvectors of the Roe linearization, i.e., if

$$v_{i+1} - v_i = \sum_{k=1}^{3} \bar{\eta}^k_{i+1/2} R^k_{i+1/2}, \tag{4.16}$$

then the modified numerical viscosity matrix becomes

$$\begin{aligned} Q_{i+1/2} = {} & \frac{b^-_{i+1/2} + b^+_{i+1/2}}{b^+_{i+1/2} - b^-_{i+1/2}} A_{i+1/2} - 2 \frac{b^+_{i+1/2} b^-_{i+1/2}}{b^+_{i+1/2} - b^-_{i+1/2}} I \\ & + \tau \delta_{i+1/2} b^+_{i+1/2} b^-_{i+1/2} \left(\frac{\eta^2_{i+1/2}}{\bar{\eta}^2_{i+1/2}} \right) B_{i+1/2}, \end{aligned} \tag{4.17}$$

where

$$B_{i+1/2} = T_{i+1/2} \begin{pmatrix} 0 & 0 & 0 \\ 0 & 1 & 0 \\ 0 & 0 & 0 \end{pmatrix} T^{-1}_{i+1/2} \tag{4.18}$$

with $T_{i+1/2} = (R^1_{i+1/2}, R^2_{i+1/2}, R^3_{i+1/2})$.

If the parameter $\delta_{i+1/2}$ is positive, then the last term on the right of (4.17) is negative and can be considered as an anti-diffusion term, which steepens contact discontinuities. $\delta_{i+1/2}$ should be chosen such that the stability condition (4.7) is valid for $k = 2$. If the numerical signal velocities are the smallest and largest eigenvalues of the Roe linearization, i.e., if

$$b^-_{i+1/2} = \min(\alpha^1_{i+1/2}, 0), \tag{4.19a}$$

$$b^+_{i+1/2} = \max(\alpha^3_{i+1/2}, 0), \tag{4.19b}$$

then the projection (3.13) is exact and therefore $\eta_{i+1/2} = \bar{\eta}_{i+1/2}$. In this case we choose

$$\delta_{i+1/2} = \frac{1}{\tau} \frac{1}{\bar{c}_{i+1/2} + |\bar{u}_{i+1/2}|}. \tag{4.20}$$

Substitution of (4.20) into (4.17) gives

$$Q_{i+1/2}(v_{i+1} - v_i) = \sum_{k=1}^{3} |\alpha^k_{i+1/2}| \bar{\eta}^k_{i+1/2} R^k_{i+1/2}, \tag{4.21}$$

where we have used (4.15), (3.14) and $\eta_{i+1/2} = \bar{\eta}_{i+1/2}$.

The numerical flux (4.1), (4.21) is the same as that of Roe's method [18]. Thus Roe's scheme can be considered as a Godunov-type method (3.7) with an anti diffusion term in the linear degenerate field.

We see that the dissipation of Roe's method (4.1), (4.21), the Godunov-type method (4.1), (4.2) (with the signal velocities (4.19)) and Godunov's method is the same across a single shock wave. We therefore expect that these methods will show a similar resolution for shock discontinuities. For a contact discontinuity the dissipation of the methods of Roe and Godunov is the same, whereas the dissipation of the Godunov-type method (4.1), (4.2) is larger. The Godunov-type method therefore spreads a contact discontinuity over more grid points.

Remark. Remember that Roe's method (4.1), (4.21) with the signal velocities (4.19) can be rewritten as

$$\begin{aligned} h_{i+1/2} = {} & \frac{b^+_{i+1/2} f(v_i) - b^-_{i+1/2} f(v_{i+1})}{b^+_{i+1/2} - b^-_{i+1/2}} \\ & + \frac{b^+_{i+1/2} b^-_{i+1/2}}{b^+_{i+1/2} - b^-_{i+1/2}} \left(v_{i+1} - v_i - \frac{\bar{c}_{i+1/2} \eta^2_{i+1/2}}{\bar{c}_{i+1/2} + |\bar{u}_{i+1/2}|} R^2_{i+1/2} \right) \end{aligned} \tag{4.22}$$

where $\bar{c}_{i+1/2}$, $\bar{u}_{i+1/2}$, $\eta_{i+1/2}$, $R^2_{i+1/2}$ are defined by (3.13), (3.14). In contrast to the commonly used flux function (4.1), (4.21) this form of the numerical flux does not require the full computation of the right eigenvectors and the decomposition (4.16).

5. Computation of the signal velocities. Harten, Lax and van Leer [10] leave open the question of how to compute approximations for the signal velocities $b^l_{i+1/2}$ and $b^r_{i+1/2}$. We now describe two algorithms for this essential part of the Godunov-type method. In the last section we saw that the most accurate resolution of shock discontinuities are obtained if we choose the smallest and largest eigenvalues of a Roe

linearization $A_{i+1/2}$ for the signal velocities. For a γ-law (ideal) equation of state a special matrix $A_{i+1/2}$ was constructed by Roe [18]. The minimal and maximal eigenvalues of this matrix are

$$b^l_{i+1/2} = \bar{u}_{i+1/2} - \bar{c}_{i+1/2}, \tag{5.1a}$$

$$b^r_{i+1/2} = \bar{u}_{i+1/2} + \bar{c}_{i+1/2}, \tag{5.1b}$$

with $\bar{c}^2_{i+1/2} = (\gamma - 1)(\bar{H}_{i+1/2} - \frac{1}{2}\bar{u}^2_{i+1/2})$. Here, $\bar{u}_{i+1/2}$ and $\bar{H}_{i+1/2}$ are the averaged velocity and averaged total enthalpy, defined by

$$\bar{u}_{i+1/2} = \frac{\sqrt{\rho_i}\, u_i + \sqrt{\rho_{i+1}}\, u_{i+1}}{\sqrt{\rho_i} + \sqrt{\rho_{i+1}}}, \tag{5.2}$$

$$\bar{H}_{i+1/2} = \frac{\sqrt{\rho_i}\, H_i + \sqrt{\rho_{i+1}}\, H_{i+1}}{\sqrt{\rho_i} + \sqrt{\rho_{i+1}}} \tag{5.3}$$

with $\rho_i H_i = e_i + p_i$. For a more general equation of state (at present) a Roe average matrix $A_{i+1/2}$ is not available in the literature and may also lead to a more complex algorithm.

Next we indicate how the Roe signal velocities (5.1) may possibly be extended to more general equations of state.

To do this we note that $\bar{c}^2_{i+1/2}$ in (5.1) can be rewritten as

$$\bar{c}^2_{i+1/2} = \frac{\sqrt{\rho_i}\, c_i^2 + \sqrt{\rho_{i+1}}\, c^2_{i+1}}{\sqrt{\rho_i} + \sqrt{\rho_{i+1}}} + \eta_\gamma(\rho_i, \rho_{i+1})(u_{i+1} - u_i)^2, \tag{5.4}$$

with

$$\eta_\gamma(\rho_i, \rho_{i+1}) = \frac{\gamma - 1}{2} \frac{\sqrt{\rho_i}\sqrt{\rho_{i+1}}}{(\sqrt{\rho_{i+1}} + \sqrt{\rho_i})^2}. \tag{5.5}$$

For most gases, the ratio of the specific heats γ is a constant between 1 and 5/3. Therefore,

$$\eta_\gamma(\rho_i, \rho_{i+1}) < \eta_2(\varphi_i, \varphi_{i+1}) = \frac{1}{2} \frac{\sqrt{\rho_i}\sqrt{\rho_{i+1}}}{(\sqrt{\rho_i} + \sqrt{\rho_{i+1}})^2} \tag{5.6}$$

and we may approximate (5.4) by

$$\bar{d}^2_{i+1/2} = \frac{\sqrt{\rho_i}\, c_i^2 + \sqrt{\rho_{i+1}}\, c^2_{i+1/2}}{\sqrt{\rho_i} + \sqrt{\rho_{i+1}}} + \eta_2(\rho_i, \rho_{i+1})(u_{i+1} - u_i)^2. \tag{5.7}$$

The signal velocities

$$b^l_{i+1/2} = \bar{u}_{i+1/2} - \bar{d}_{i+1/2}, \tag{5.8a}$$

$$b^r_{i+1/2} = \bar{u}_{i+1/2} + \bar{d}_{i+1/2} \tag{5.8b}$$

are also well defined for a general convex equation of state, since the sound speed c_i can be computed directly from

$$c_i^2 = \tau^2(pp_e - p_\tau) \qquad (\tau = 1/\rho). \tag{5.9}$$

Since

$$\bar{d}_{i+1/2} > \bar{c}_{i+1/2}, \tag{5.10}$$

these signal speeds satisfy the stability requirement (4.6) for any γ-law gas. We cannot yet answer the corresponding question for a more general equation of state.

Remark. Lax proved [22, Thm. 17.16] that for weak shocks, the shock speed s is well approximated (up to second order terms in the shock strength) by the average of the two characteristic speeds which impinge on the shock from both sides. This holds for a general convex equation of state.

A short calculation shows that

$$\bar{u}_{i+1/2} = \tfrac{1}{2}(u_i + u_{i+1}), \tag{5.11a}$$

$$\bar{d}_{i+1/2} = \tfrac{1}{2}(c_i + c_{i+1}), \tag{5.11b}$$

up to second-order terms in the shock strength.

Thus, for sufficiently weak shocks, the physical signal velocities are well approximated by the numerical signal velocities (5.8), (5.7), (5.2), even for a general convex equation of state.

6. Numerical results. We have used the numerical method (3.6), (3.7) together with the Roe-signal velocities (5.1) and the signal velocities (5.8). We will refer to the first version as the HLLR-method and denote the second version as the HELL-method.

A. One-dimensional problems. The first numerical experiment was used by Sod [24] to compare a variety of new and established finite-difference schemes. This test problem is a standard shock-tube problem for the conservation laws (2.2). The initial conditions are

$$\begin{aligned} &x < 0.5, && 0.5 < x, \\ &\rho_l = 1.0, && \rho_r = 0.125, \\ &u_l = 0.0, && u_r = 0.0, \\ &p_l = 1.0, && p_r = 0.1. \end{aligned} \tag{6.1}$$

In the calculation we have used 100 cells with $\Delta = 0.01$ and CFL $= 0.8$. The numerical solution is evaluated after 50 timesteps.

Figure 4 shows the results of the HLLR scheme. The corners at the endpoints of the rarefaction wave are rounded. The constant state between the contact discontinuity and the shock has been realized. The contact discontinuity is spread over sixteen to eighteen zones, while the transition of the shock occupies only two to four zones.

For comparison, Godunov's method is shown in Fig. 5. To compute the full Riemann problem we used the iteration method described in [6]. The plot is almost equal to that of Fig. 4. Only the right corner of the rarefaction wave is slightly less rounded and the contact discontinuity is slightly less smeared.

Figure 6 represents the results of the Roe scheme. The plot is the same as in Fig. 5, except that the right corner of the rarefaction wave is slightly more rounded.

The results for the HELL-method (not shown) are identical to the plot of Fig. 4.

The second test problem was used by Lax in [11]. The initial conditions for this Riemann problem are

$$\begin{aligned} &x < 0.5, && 0.5 < x, \\ &\rho_1 = 0.445, && \rho_r = 0.5, \\ &u_1 = 0.698, && u_r = 0.0, \\ &p_l = 3.528, && p_r = 0.571. \end{aligned} \tag{6.2}$$

Other numerical experiments with this problem are reported in [9].

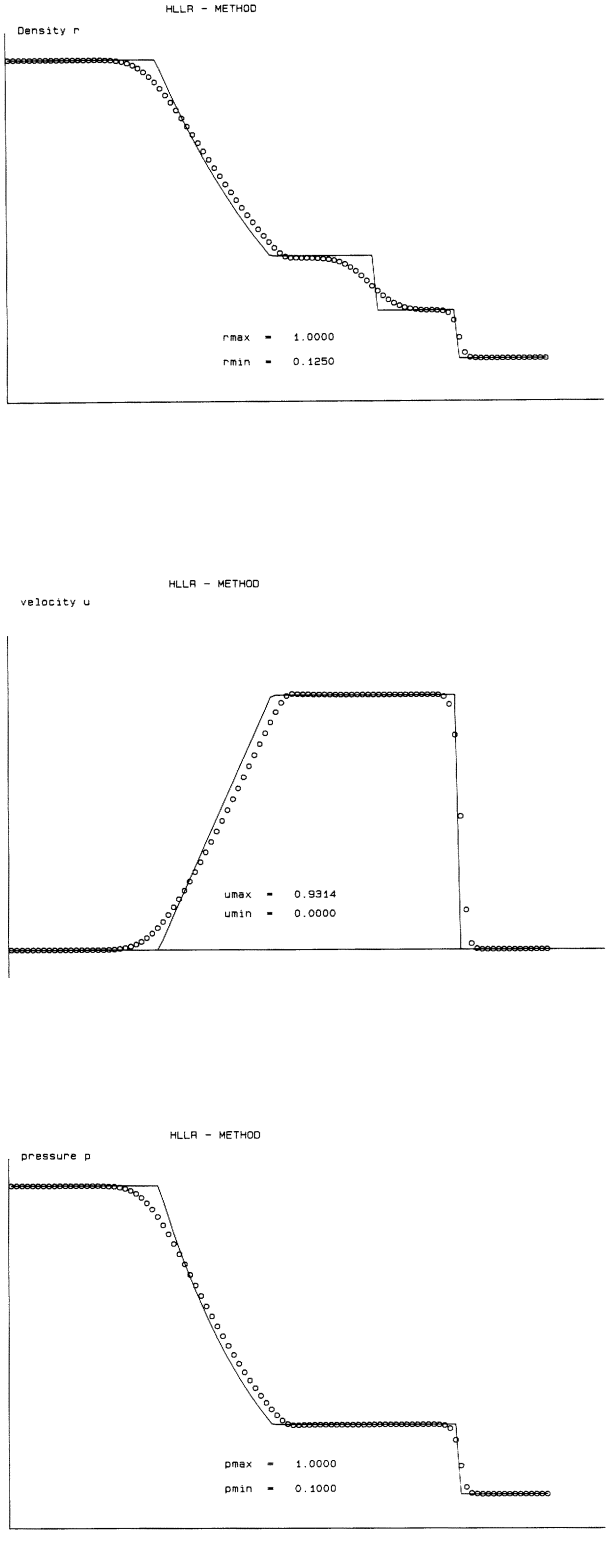

FIG. 4. *The* HLLR *scheme for Sod's problem.*

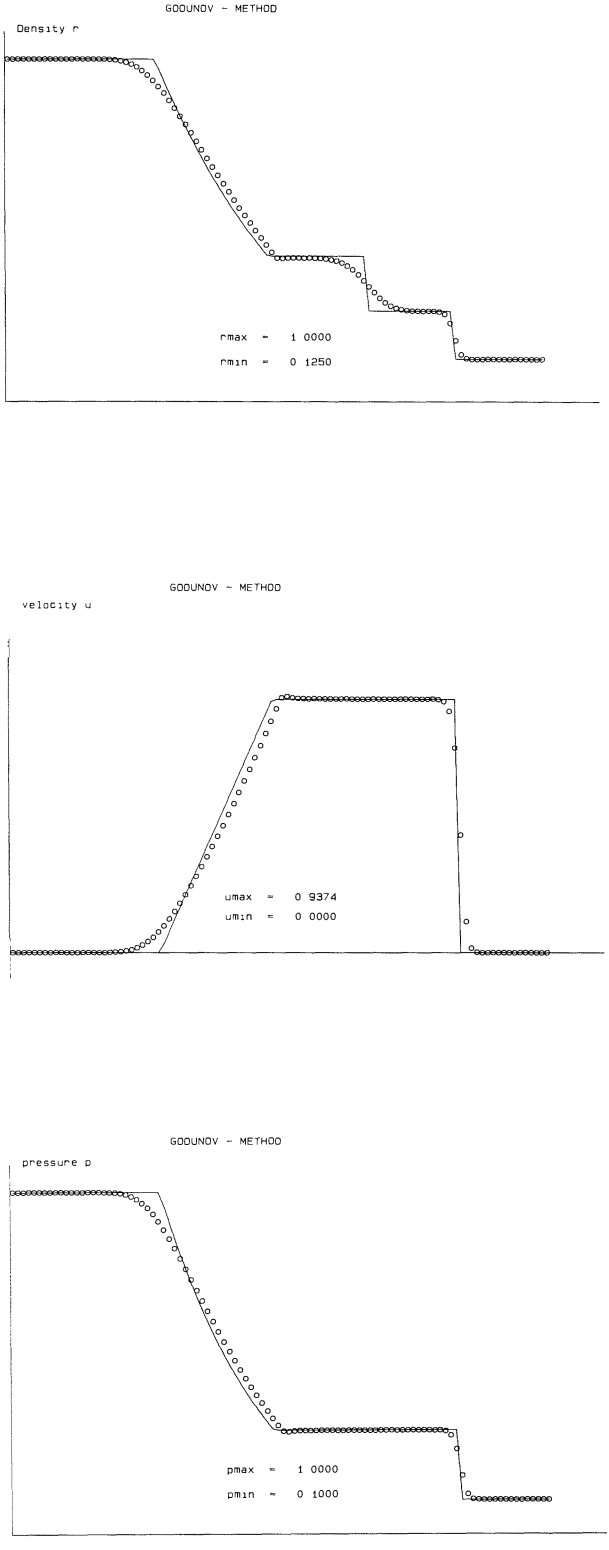

FIG. 5. *Godunov's scheme for Sod's problem.*

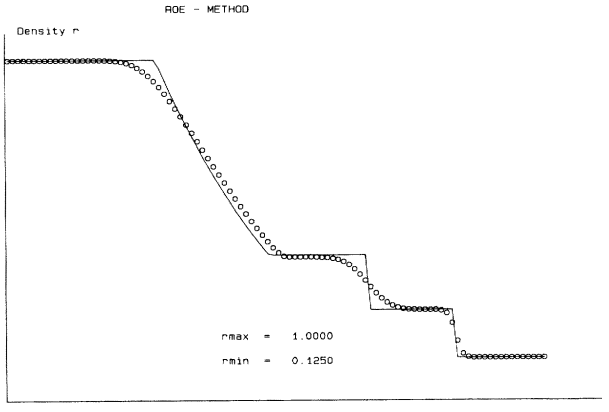

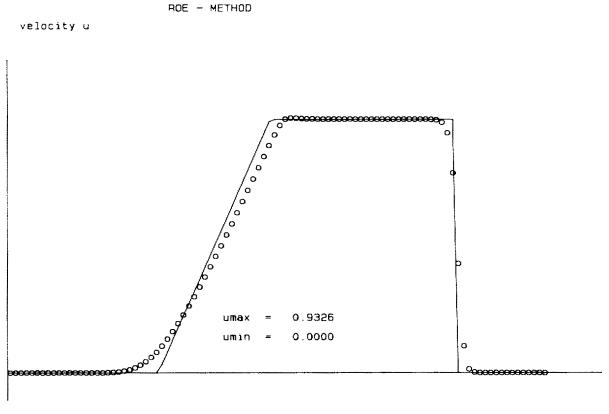

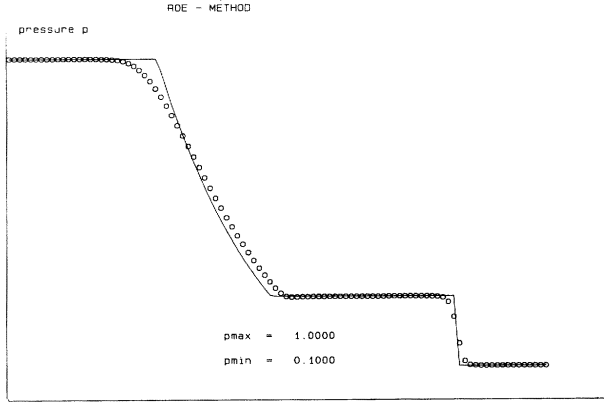

FIG. 6. *Roe's scheme for Sod's problem.*

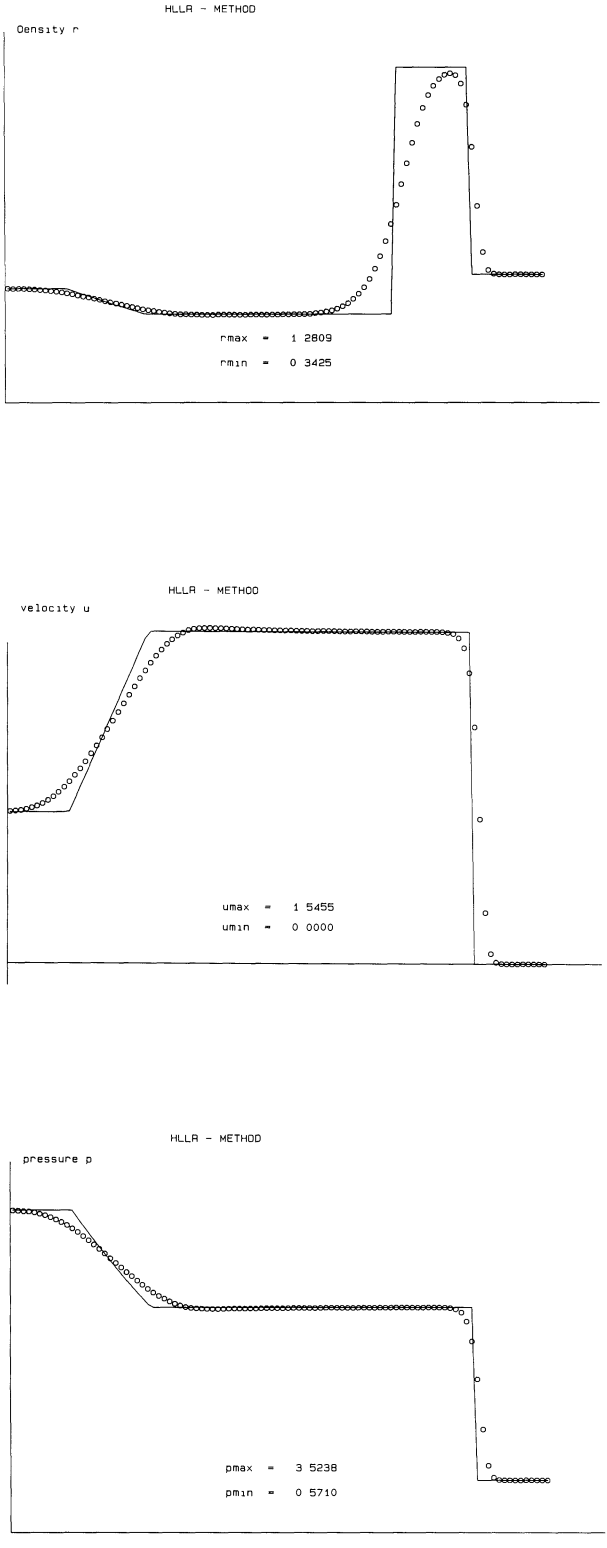

FIG. 7. *The* HLLR *scheme for Lax's problems.*

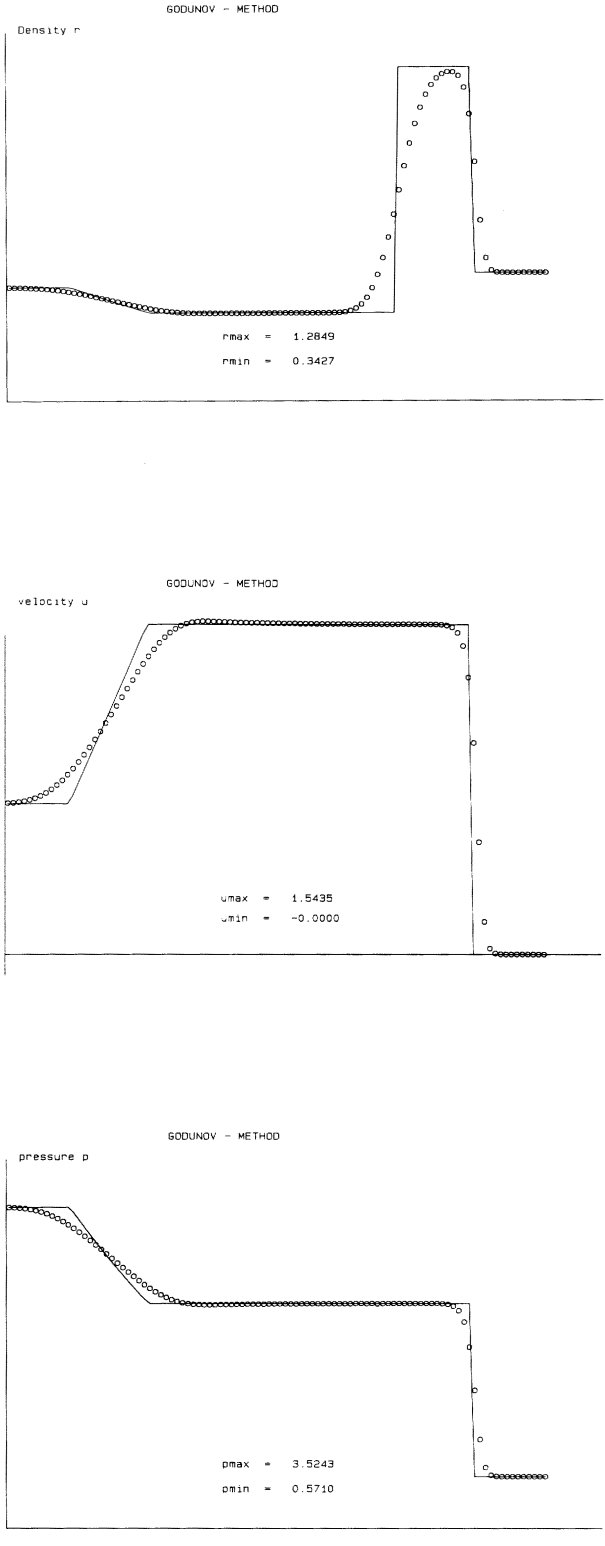

FIG. 8. *Godunov's scheme for Lax's problem.*

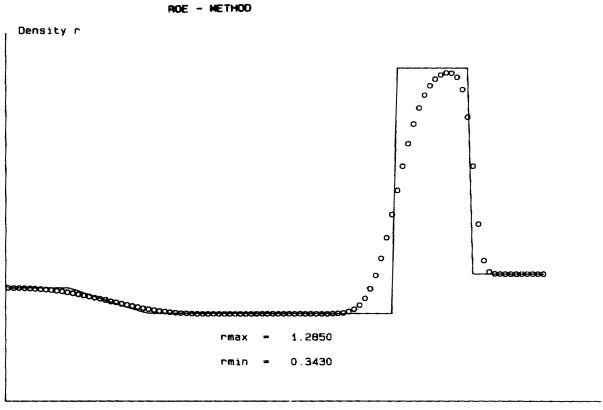

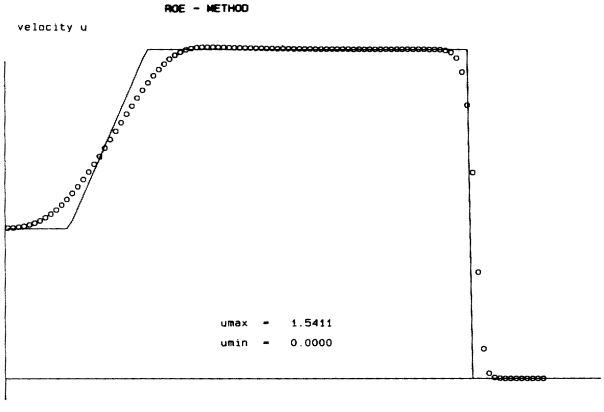

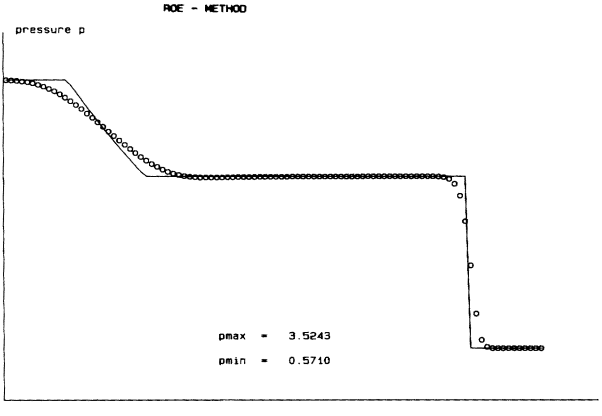

FIG. 9. *Roe's scheme for Lax's problem.*

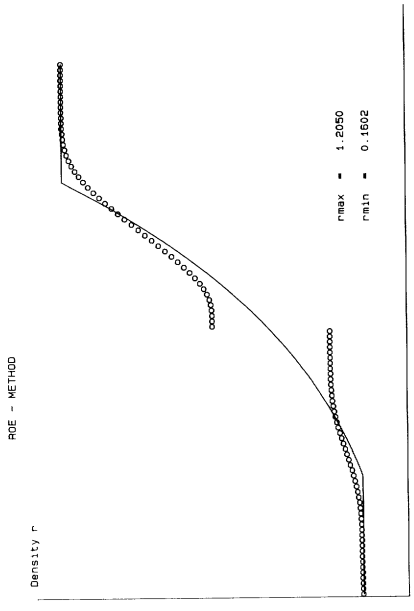

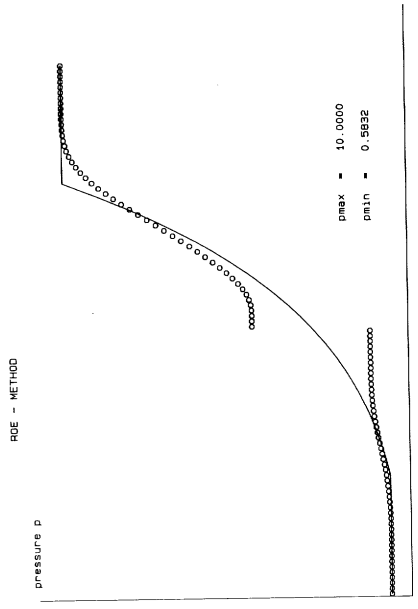

FIG. 11

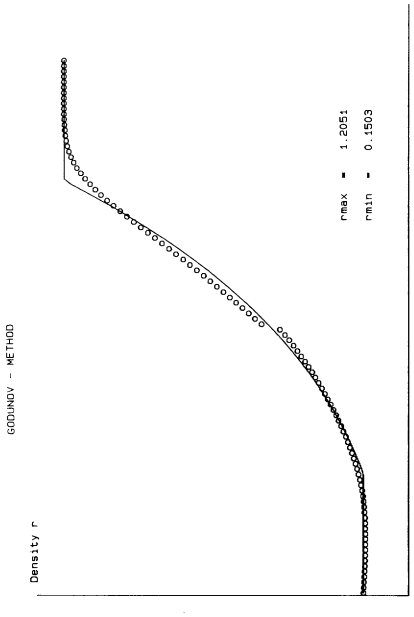

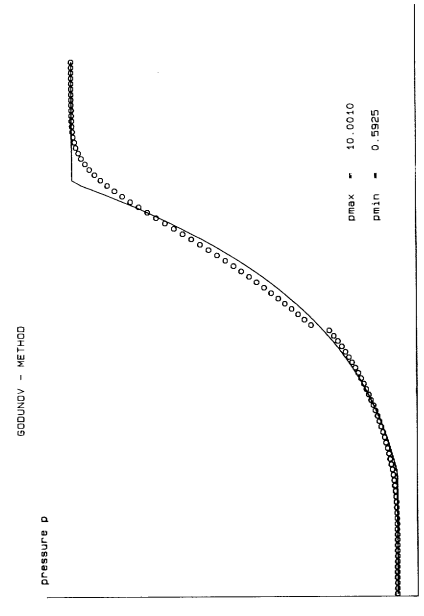

FIG. 10

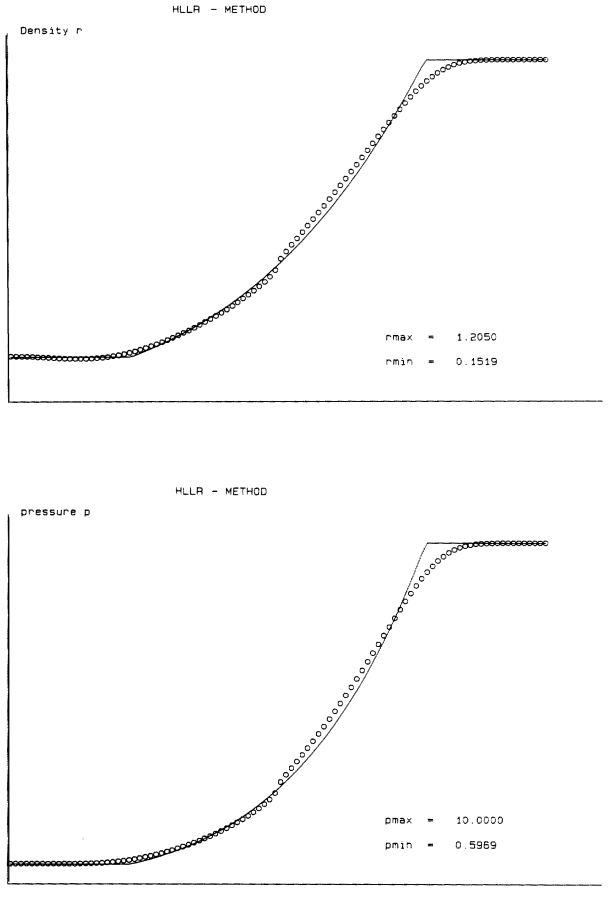

FIG. 12

FIGS. 10-12. *Godunov's, Roe's and the* HLLR *scheme with the modified signal velocities* (4.11) *for a rarefaction wave with sonic point.*

In Figs. 7 and 8 we show the results of applying the HLLR-method and Godunov scheme to this problem. The only significant difference occurs in the resolution of the contact discontinuity. The HLLR-method requires about three more points for the transition.

Figure 9 represents the result for Roe's scheme. The plot is nearly identical to that of the Godunov scheme.

Next we test for the resolution of an entropy violating stationary shock by considering a Riemann problem where the states v_l and v_r are connected by a rarefaction wave. Fixing the state v_r by $\rho_r = 1.205$, $u_r = 0.0$, $p_r = 10$ and $c_l = (3-\gamma)/(\gamma+1)c_r$, we determine the state v_l by

$$\rho_1 = \left(\frac{c_l}{c_r}\right)^{2/(\gamma-1)} \cdot \rho_r,$$

$$u_1 = -(c_r + c_1), \tag{6.3}$$

$$p_1 = \rho_1 c_l^2/\gamma.$$

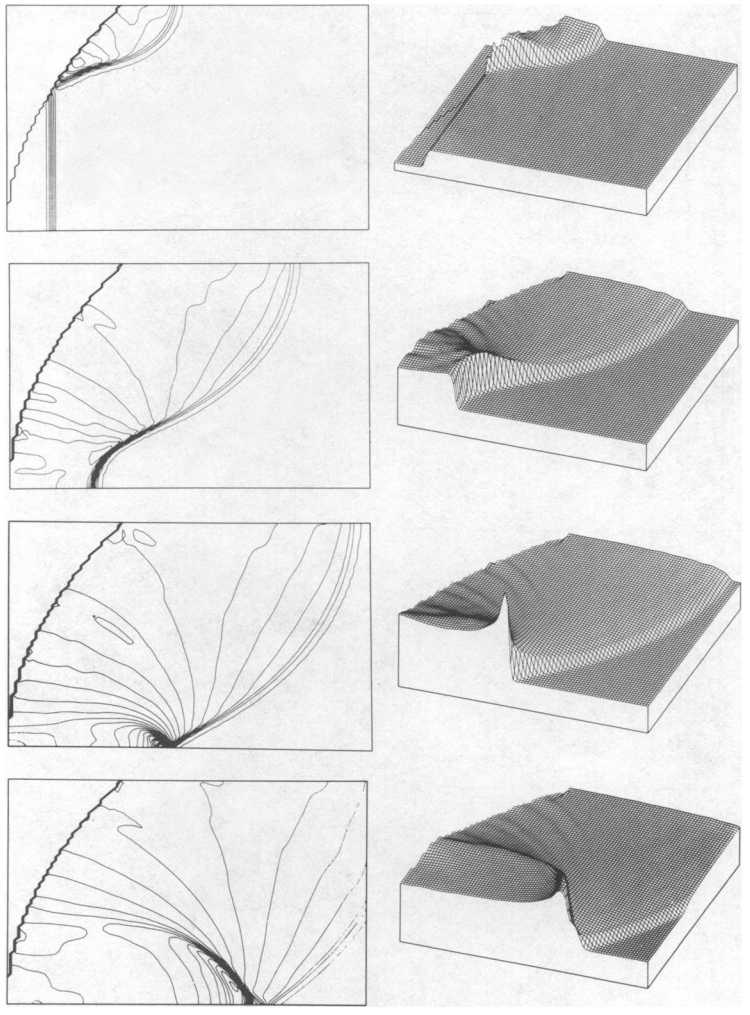

FIG. 13. *Second order extension of Godunov's method for the shock focusing problem.*

The calculations in Figs. 10–12 were performed with 80 timesteps and 100 cells for a CFL number of 0.8. Godunov's scheme (Fig. 10) breaks up the initial discontinuity. The occurrence of the "kink" in the solution is well known. Figure 11 shows that Roe's scheme admits an entropy violating stationary shock. The same entropy violation occurs for the HLLR scheme. In Fig. 12 we present the results for the HLLR scheme, with the modified signal velocities (4.11). The plot is now nearly identical to that of the Godunov scheme. The "kink" in the solution is even smaller. The modification (4.11) does not alter the numerical results for the two preceding test problems. A similar modification can be used for Roe's scheme, with the numerical flux in the form (4.22).

We remark that the occurrence of a nonphysical discontinuity is only possible if there is a sonic point in an expanding region.

B. A two-dimensional problem. The test problem is the focusing of a plane shock wave in air ($\gamma = 1.4$) by a parabolic reflector. The Godunov-type methods we have

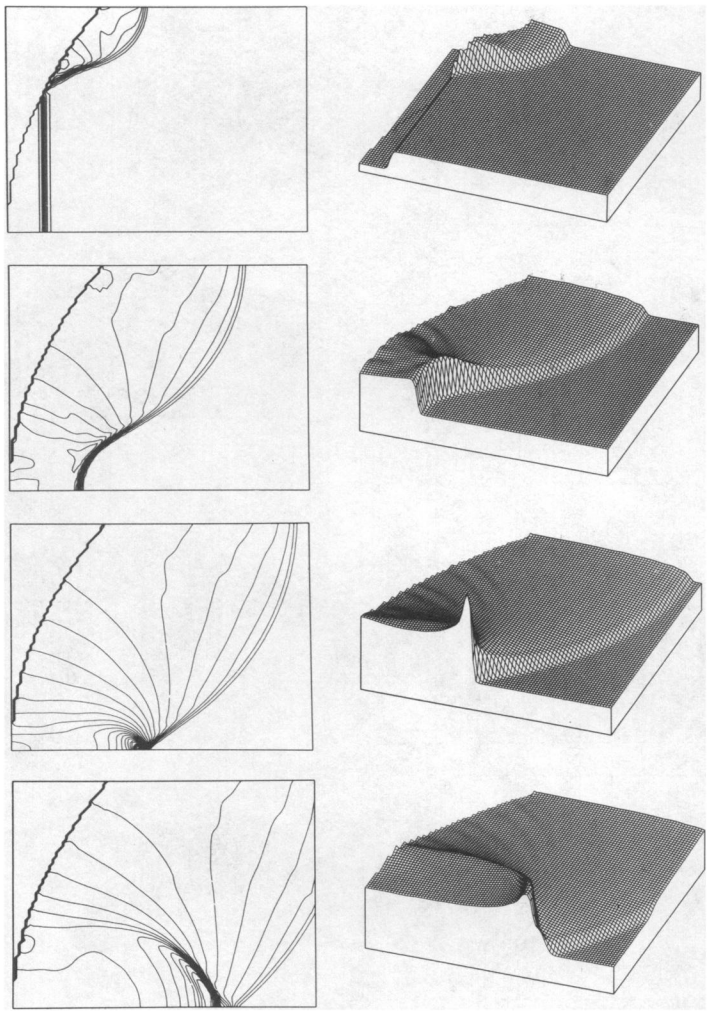

FIG. 14. *Second order extension of the* HLLR *scheme for the shock focusing problem.*

described are only first-order accurate in smooth parts of the solution. For the application to "real world" problems first-order accuracy is not sufficient. To compute the numerical solution of the focusing of a plane shock wave, we have incorporated Roe's Riemann solver and the HLLR-Riemann solver in the second-order extension of Godunov's method, described by Colella and Glaz in [3].

The numerical calculations were made in two space dimensions by extending the one-dimensional method via a fractional step method. The Mach number of the incident shock wave is 1.1. In the numerical calculation, the shape of the reflector is approximated by a stepwise wall to apply simple reflecting boundary conditions [2]. Because the considered flow problem is symmetrical, only the upper halfplane of the flow is computed. The halfplane was discretized by a 90×90 grid. At the reflector boundary and the axis of symmetry, the reflection boundary condition is applied. At the other boundaries of the grid no reflection is assumed. All calculations were done on a Cyber 175 computer.

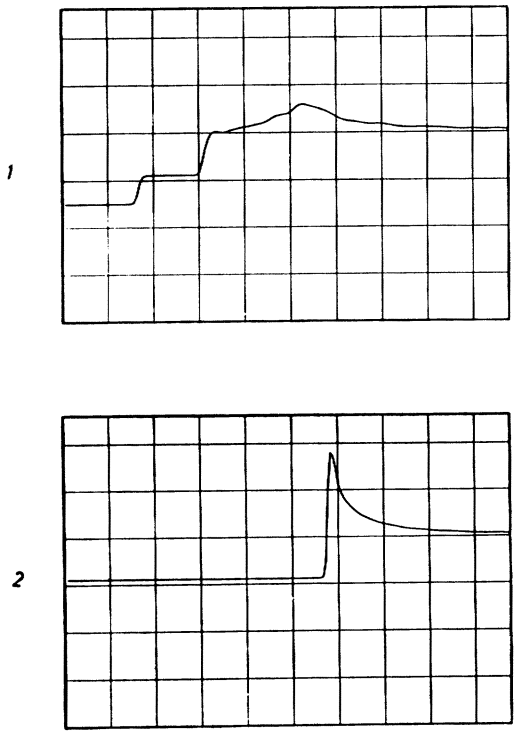

FIG. 15. *Pressure history for a second-order extension of Godunov's method.*

A more detailed description of this test problem is given by Olivier and Grönig in [16]. They performed calculations with the Random Choice Method and compared the numerical results for the shock focusing problem with experimental data. Experimental and numerical studies of shock wave focusing in water are performed in [21].

Figure 13 represents the results for the PLM-method [3] with the full solution to the Riemann problem. The Riemann problem was computed by the iterative method [24]. The pressure contours are shown in the process of reflection from the wall, after reflection from the wall, at the moment of and after focusing.

Figure 14 shows the result for the PLM-method with the HLLR-Riemann solver. The pressure contours are very similar.

More particular information can be obtained from Figs. 15–17. The pressure histories close to the reflector are shown (see [16] for details of the location). No difference was found between the pressure histories of the PLM-method with the full solution to the Riemann problem (Fig. 15) and with Roe's Riemann solver (Fig. 16). Figure 17 represents the pressure histories of the PLM-method with the HLLR-Riemann solver. The shock waves in the first pressure history are the same as in Fig. 15. The maximum in Fig. 15 is slightly higher. In the second pressure history there is a slight "kink" behind the shock wave, which does not occur in Fig. 15. The peak is slightly higher for the HLLR-Riemann solver but is more rounded.

7. Discussion and conclusion. In this paper we have shown that it is sufficient to derive a numerical approximation for the smallest and largest physical signal velocity in the Riemann problem to obtain an efficient Riemann solver for gas dynamics.

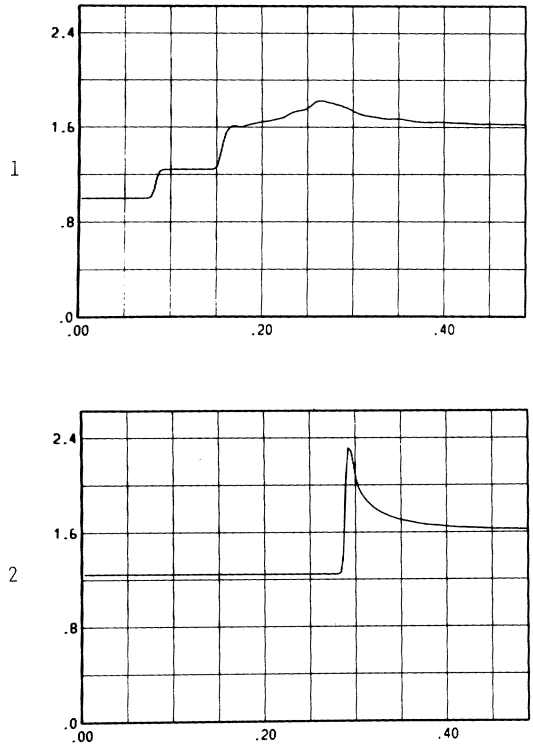

FIG. 16. *Pressure history for a second-order extension of Roe's method.*

A stability condition for the numerical signal velocities was derived in § 4. Here we also demonstrate a relationship between the signal velocities and the dissipation contained in the corresponding Godunov-type method.

The computation of the signal velocities for general (convex) equation of state was discussed in § 5.

The great advantage of the Riemann solver (3.3) is its simplicity. The approximation substantially reduces the program complexity while retaining essential features of Godunov's method, especially the accurate approximation of shock waves. Furthermore, a vectorizable version is easily obtained.

A drawback of the Godunov-type method (3.6), (3.7) is that the resolution of a nearly stationary contact discontinuity requires more grid points as Godunov's method.

We showed that this problem can be overcome by introducing an antidiffusion term in the linear degenerate field. If we choose the smallest and largest eigenvalues of the Roe linearization [18] for the numerical signal velocities, then the Godunov-type method (3.6) with the modified numerical flux function (3.15), (4.20) becomes identical with Roe's flux function. Thus we obtained a new interpretation of Roe's scheme [18].

The successful application to the shock focusing problem shows the usefulness of the Riemann solver in a higher-order Godunov-type scheme.

Acknowledgments. The author thanks the Stosswellenlabor of the Rheinisch-Westfälische Technische Hochschule Aachen for making available the plotsoftware for the

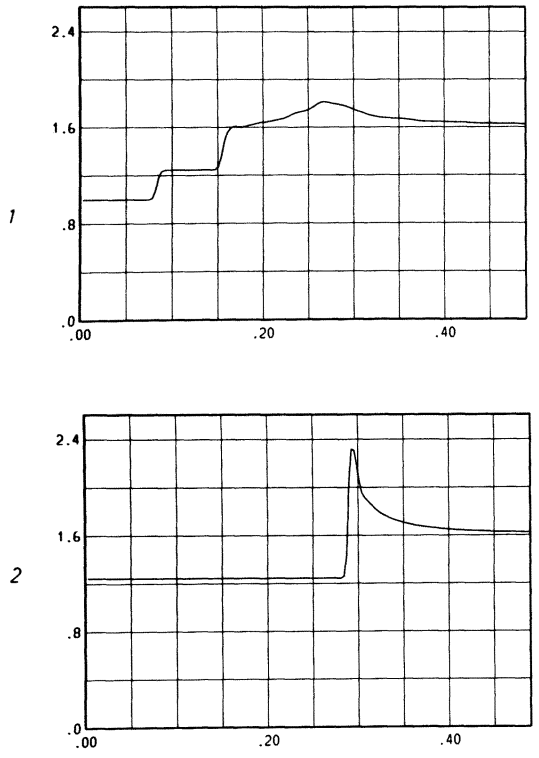

FIG. 17. *Pressure history for a second-order extension of the* HLLR *scheme.*

shock focusing problem. Special thanks are to Dr. M. Sommerfeld from the Stosswellenlabor, for his help in the two-dimensional shock focusing calculation and the provision of the two-dimensional PLM-code.

REFERENCES

[1] P. COLELLA AND P. R. WOODWARD, *The piecewise-parabolic method* (PPM) *for gas-dynamical simulations*, J. Comput. Phys., 54 (1984), pp. 174–201.

[2] P. COLELLA, *A direct Eulerian muscle scheme for gas dynamics*, SIAM J. Sci. Statist. Comput., 6 (1985), pp. 104–117.

[3] P. COLELLA AND H. M. GLAZ, *Efficient solution algorithms for the Riemann problem for real gases*, J. Comput. Phys., 59 (1985), pp. 264–289.

[4] R. COURANT AND K. O. FRIEDRICHS, *Supersonic Flow and Shock Waves*, Wiley Interscience, New York, 1948.

[5] J. K. DUKOWICZ, *A general, non-iterative Riemann solver for Godunov's method*, J. Comput. Phys., 61 (1985), pp. 119–137.

[6] B. EINFELDT, *Ein schneller Algorithmus zur Lösung des Riemann Problems*, Computing, 39 (1987), pp. 77–86.

[7] S. K. GODUNOV, *A difference scheme for numerical computation of discontinuous solutions of equations of fluid dynamics*, Mat. Sb., 47 (1959), pp. 271–290.

[8] A. HARTEN, *On a class of high resolution total-variation-stable finite-difference schemes*, this Journal, 21 (1984), pp. 1–23.

[9] ———, *High resolution schemes for hyperbolic conservation laws*, J. Comput. Phys., 49 (1983), pp. 357–393.

[10] A. HARTEN, P. D. LAX AND B. VAN LEER, *On upstream differencing and Godunov-type schemes for hyperbolic conservation laws*, SIAM Rev., 25 (1983), pp. 35–61.

[11] P. D. LAX, *Weak solutions of nonlinear hyperbolic equations and their numerical computation*, Comm. Pure Appl. Math., 7 (1954), pp. 159–193.

[12] B. VAN LEER, *Towards the ultimate conservative difference scheme*, IV. *A new approach to numerical convection*, J. Comput. Phys., 23 (1977), pp. 276–299.

[13] ———, *Towards the ultimate conservative difference schemes* V. *A second order sequel to Godunov's method*, J. Comput. Phys., 32 (1979), pp. 101–136.

[14] ———, *On the relation between the upwind-differencing schemes of Godunov, Engquist–Osher and Roe*, SIAM J. Sci. Statist. Comput., 5 (1984), pp. 1–20.

[15] S. OSHER AND F. SOLOMON, *Upwind difference schemes for hyperbolic systems of conservation laws*, Math. Com., 38 (1982), pp. 339–374.

[16] H. OLIVIER AND H. GRÖNIG, *The random choice method applied to two-dimensional shock focussing and diffraction*, J. Comput. Phys., 63 (1986), pp. 85–106.

[17] M. PANDOLFI, *A contribution to numerical prediction of unsteady flows*, AIAA J., 22 (1984), pp. 602–610.

[18] P. L. ROE, *Approximate Riemann solvers, parameter vectors, and difference schemes*, J. Comput. Phys., 53 (1981), pp. 357–372.

[19] ———, *The Use of the Riemann Problem in Finite-Difference Schemes*, Lecture Notes in Physics 141, Springer-Verlag, New York, 1981, pp. 354–359.

[20] ———, *Some contributions to the modeling of discontinuous flows*, Lecture Notes in Applied Mathematics 22, Springer-Verlag, New York, 1985, pp. 163–193.

[21] M. SOMMERFELD AND H. M. MÜLLER, *Experimental and numerical studies of shock wave focusing in water*, Experiments in Fluids, submitted.

[22] J. SMOLLER, *Shock Waves and Reaction-Diffusion Equations*, Springer-Verlag, New York, 1983.

[23] G. A. SOD, *Numerical Methods in Fluid Dynamics*, Cambridge University Press, Cambridge, 1985.

[24] ———, *A survey of several finite difference methods for systems of nonlinear hyperbolic conservation laws*, J. Comput. Phys., 27 (1978), pp. 1–31.

[25] P. WOODWARD, P. COLELLA, B. A. FRYXELL AND K. H. WINKLER, *An implicit–explicit hybrid method for Lagrangian hydrodynamics*, J. Comput. Phys., 63 (1986), pp. 283–310.

[26] P. WOODWARD AND P. COLELLA, *The numerical simulation of two-dimensional fluid flow with strong shocks*, J. Comput. Phys., 54 (1984), pp. 115–173.